Efficient wave-equation-based forward modeling of time-lapse post-stack seismic images with illumination variations

Wilson S. Duarte*, David Riffault and Huub Douma (CGG)

This paper was prepared for presentation during the 15th International Congress of the Brazilian Geophysical Society held in Rio de Janeiro, Brazil, 31 July to 3 August, 2017.

Abstract

In time-lapse feasibility studies one of the objectives is to test the impact on the image of different production scenarios to determine the optimal timing between time-lapse seismic monitoring experiments. The ability to model illumination variations due to a complex overburden as well as the acquisition geometry benefits such analysis. We show that point-spread-function-based forward modeling allows incorporation of such variations into the modeled images. The point-spread functions are here calculated using the two-way wave-equation and can thus be used to model images as if they were obtained using RTM. We illustrate the method using 2D synthetic examples with mild velocity variations. Because point-spread-functions have a finite extent, the method can efficiently forward model images from a changing reflectivity model. The method is expected to benefit time-lapse feasibility studies for pre-salt reservoirs offshore Brazil, because such reservoirs are buried underneath a complex overburden and illuminated using imperfect acquisition geometries.

Introduction

Time-lapse (4D) seismic data plays an important role in production monitoring of hydro-carbon reservoirs (e.g., Hatchell *et al*., 2002 and Formento *et al*., 2007). In 4D feasibility studies, simulator-to-seismic workflows are routinely used to estimate the seismic response due to changes in the reservoir models. These simulators can help decide the optimal timing for 4D monitoring seismic surveys and update the reservoir parameters (porosity, saturation and pressure) so that they match the 4D seismic data as well as the production history (Allo *et al*., 2013).

To calculate the synthetic seismic traces, forward modeling is currently mostly based on a 1D convolution of the reflectivity model with a stationary or space-variant wavelet to generate synthetic traces in the time domain. The advantage of this method is its computational efficiency (Toxopeus *et al*., 2008). Historically, this facilitated the use of computationally expensive non-linear inversion algorithms to invert seismic images for detailed reservoir models.

The 1D convolutional method, however, is strictly valid for horizontally layered models only (e.g., Lecomte, 2008 and Lecomte *et al*., 2016) and models the seismic data in the time-domain. In order to overcome this limitation, knowing that computational power has substantially improved over the past decades, Lecomte (2004 and 2008) and Toxopeus *et al*. (2008) devised a depth-domain method using multi-dimensional filtering with point-spread functions (PSFs). A PSF determines what a point in the reflectivity model looks like in the image domain. It incorporates the illumination variations due to a complex overburden (i.e. the velocity model) and acquisition geometry. Because the PSFs are calculated in the depth-domain they also incorporate the changing wavelength due to the changing velocity.

PSFs can be calculated in various ways using, e.g., ray-tracing, one-way modeling operators, or two-way wave-equation-based operators. In the context of time-lapse forward modeling of seismic images from changes in reservoir parameters, it is preferable to calculate the PSFs using the same operators that are used to calculate the image from the field data. In that way the forward modeling becomes imaging-consistent.

The concept of a PSF has its roots in model resolution in inverse theory (e.g., Parker, 1994). In seismic imaging/inversion an early use of it can be found in Humphreys *et al*. (1984) who used it to de-blur a tomographic image. Recently it has been used in the context of inverting for elastic parameters in reservoir characterization studies (Fletcher *et al*., 2012, Archer *et al*., 2013 and Letki *et al*., 2015), as well as to perform de-ghosting in the image domain (Caprioli et al., 2014 and Caprioli et al., 2015).

In this paper, we present an example of forward modeling of time-lapse post-stack depth-domain seismic images using PSFs. The PSFs are here calculated using two-way wave-equation-based modeling and migration operators, using the method from Fletcher *et al*. (2012). The example we show highlights the ability of the method to incorporate illumination variations due to the acquisition geometry and the velocity model, into the forward modeling of a time-lapse seismic response from a changing reservoir. We anticipate this method to be beneficial for 4D feasibility studies of pre-salt reservoirs off-shore Brazil, because these reservoirs are buried underneath a complex overburden of salt and carbonates and imaged using acquisition geometries with imperfect illumination (such as narrow-azimuth streamer acquisitions).

Method

Based on a single scattering assumption (i.e. Born modeling), the dependence of the data on the reflectivity can be written as

$$d = M\,r \tag{1}$$

where r is a vector holding the reflectivity, d is a vector holding the data, and M is the single scattering (i.e. Born) modeling operator. The modeling operator depends on both the background velocity model as well as the acquisition geometry. The migration operator can be written as M^*, where the star denotes the adjoint operator. Hence, the estimated reflectivity after migration can be written as

$$\hat{r} = M^*\,d \tag{2}$$

where $\hat{r}$ denotes the estimated reflectivity (i.e. the image). Using equation (1) we then get

$$\hat{r} = M^* M\,r := H\,r \tag{3}$$

where we defined $H{:} = M^*M$. The operator H is known as the Hessian operator. Equation (3) determines the relation between the actual reflectivity r in the earth and the estimated reflectivity $\hat{r}$ obtained after migration.

Writing the reflectivity r as a weighted sum of point-scatterers $r_i = \sum_j r_j \delta_{ji}$, with δ_{ji} the Kronecker delta function, we find that the estimated reflectivity $\hat{r}$ can be written as

$$\hat{r}_i = \sum_j r_j P_{ij} \tag{4}$$

where we defined the PSF P_{ij} as

$$P_{ij} = \sum_k H_{ik}\delta_{kj}\ , \tag{5}$$

which shows that the PSF at location i in the model, due to a point-scatterer at location j in the model, equals the j-th column from the Hessian matrix. Equation (4) indicates that the estimated reflectivity can thus be modeled as a weighted sum of PSFs (Lecomte, 2004 and Toxopeus *et al.*, 2008).

The Hessian depends only on the modeling operator and its adjoint. Given that the modeling operator depends on the background velocity model and the acquisition geometry, but not on the reflectivity model, it follows that the PSF is independent of the reflectivity model. This is a direct result of the Born modeling in equation (1). This implies that the PSF only needs to be calculated once for a given background velocity model and acquisition geometry, but does not need to be updated when the reflectivity model changes (Toxopeus *et al.*, 2008). That means that given a base reflectivity $\hat{r}^0$ and a reflectivity perturbation Δr, we can model the image $\hat{r}^1$ from the perturbed reflectivity using

$$\hat{r}_i^1 = \hat{r}_i^0 + \sum_j \Delta r_j P_{ij}\ . \tag{6}$$

This makes the method particularly attractive for inversion-based methods such as reservoir characterization. Equation (6) implies that the image due to a changing reflectivity model can be updated using a local calculation only. Changes in the acquisition geometry as well as the (background) velocity model, however, would require re-calculation of the PSFs.

The challenge is the efficient calculation of the PSF since it requires, in principle, one wavefield modeling as well as one migration for each point in the reflectivity model. This means that the computation of the PSF would cost as many imaging and wavefield modelings as there are points in the reservoir model, making it prohibitively expensive. We address this challenge using the method

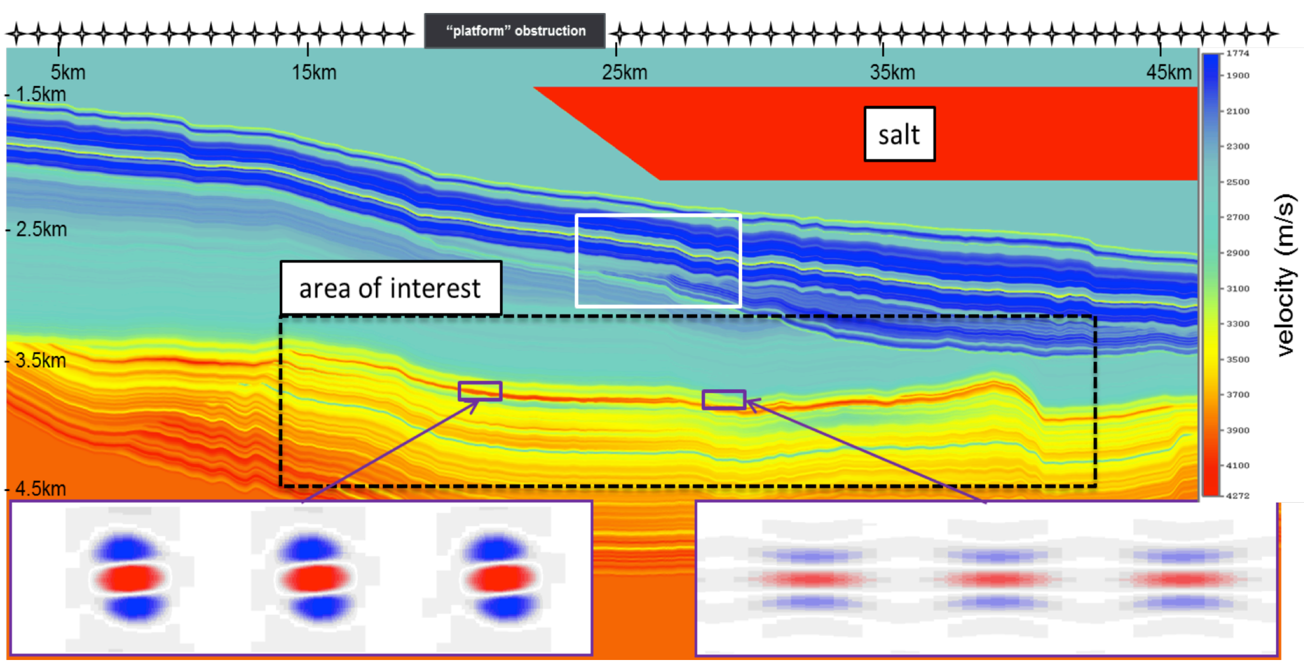

Figure 1 – Velocity model used for this study. The salt overhang is used to create illumination variations in the area below the salt compared to areas not underneath the salt. Furthermore, a "platform" obstruction was used as an area without any sources and receivers, to create further illumination variations due to obstructions in the acquisition geometry. The inset PSFs highlight the illumination variations for an area below (right) and not below the salt (left).

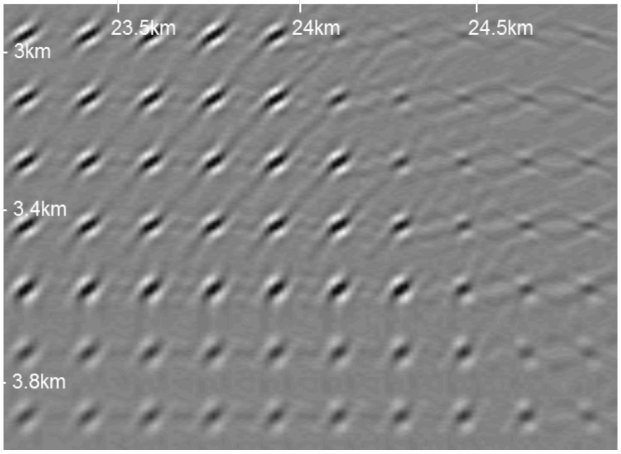

Figure 2 – PSFs from a uniform grid of point scatterers in the area indicated by the white box in Figure 1.

of Fletcher et al. (2012) that calculates the PSFs for a sparse set of points in the model (sparse enough such that their PSFs interfere only negligibly), followed by interpolation. Hence, the cost of the calculation of the PSFs is just one wavefield modeling, one migration, followed by interpolation. Because in this paper we focus on post-stack forward modeling only, the interpolation is done after stacking.

Results

Figure 1 shows the 2D synthetic velocity model that was used throughout this work. The velocity contrasts in this model are realistic, as they were modeled based on observations from field data. We used a salt body to introduce illumination variations due to the velocity model. Therefore, as we go from left to right in the subsurface, illumination is varying from good illumination to poorer illumination. This is highlighted by the PSFs. Furthermore the model contains three low impedance areas inside the dashed box that simulate hydrocarbon reservoirs.

Figure 2 shows PSFs from a uniform grid of point scatterers in the area indicated by the white box in Figure

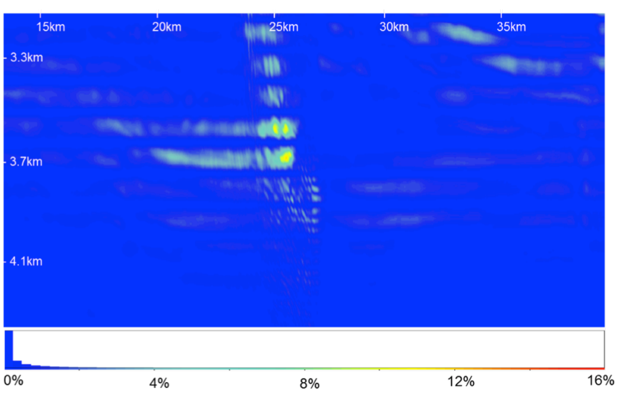

Figure 3 – Interpolation error for the area indicated by the black dashed line in Figure 2. Overall the quality of the interpolation is very high throughout the whole area. Where the illumination changes relatively rapidly, some small errors can be observed.

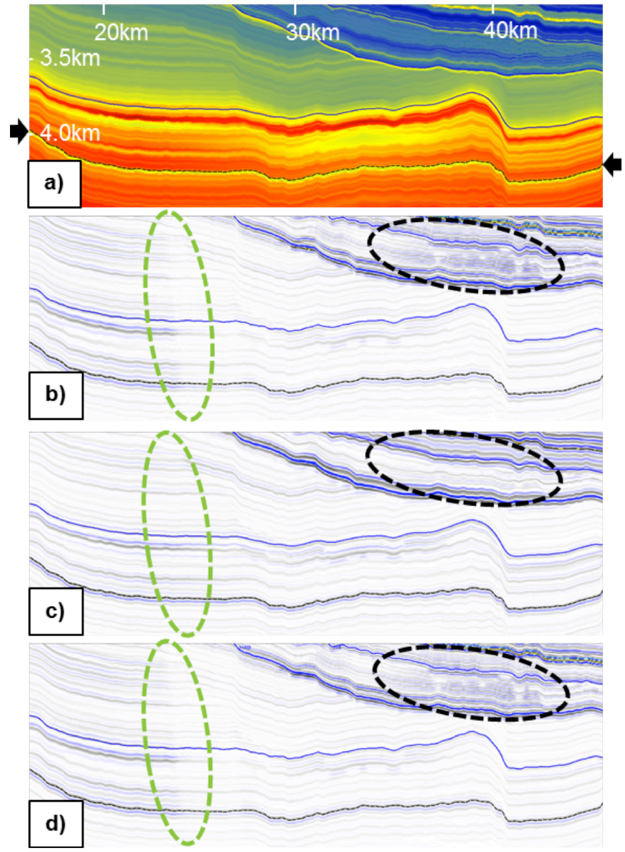

Figure 4 – Velocity model zoom from the area indicated by the dashed black line in Figure 1 (a), image obtained using RTM (b), 1D convolutional forward modeling (c), and PSF-based forward modeling (d).

1. The changing shapes and amplitudes of the PSFs as a function of position indicate that the illumination is changing quite rapidly in this area. These PSFs are the result from one modeling followed by a migration of a uniform grid of point scatterers. These PSFs form the input to the interpolation to obtain PSFs for each point in the model.

To estimate the accuracy of the interpolation we calculated a benchmark set of PSFs where one PSF was explicitly calculated for each point in the model using many forward modelings and migrations. Then these benchmark PSFs were compared to the interpolated PSFs. To quantify the error in the interpolation we used the RMS difference between the interpolated and benchmark PSFs, and compared that to the RMS of the benchmark PSF at that location. Figure 3 shows the resulting percentage errors for each point in the model in the area indicated by the dashed black box in Figure 1. Overall the errors are small indicating a good quality interpolation.

To verify that PSFs can model seismic data including illumination variations, we compared an image obtained using 1D convolution with that from PSF-based forward modeling. Figure 4a shows again the velocity model from the area inside the dashed black box inside Figure 1. Figure 4b shows the result of migrating the modeled

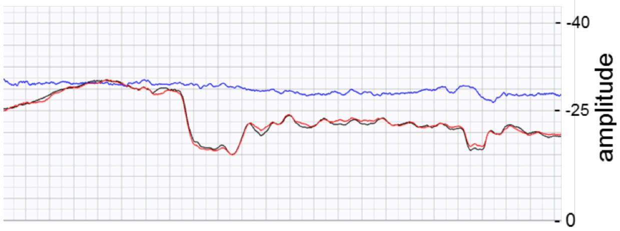

Figure 5 – Amplitude extracted along the thin reservoir indicated by the black arrows in Figure 4a for the RTM image (black), 1D convolution (blue) and the PSF-based forward modeling (red).

synthetic data using reverse-time migration. This image serves as a reference to gauge the accuracy of the PSF-based forward modeling method. We highlight two areas to analyze the differences between both methods. In the area indicated by the green dashed ellipse, we observe strong amplitude changes due to illumination variations. Furthermore, in the area indicated by the black dashed ellipse, we see small scale reflectivity in the image due to low velocities and thus a changing wavelength.

Figures 4c and 4d show the result from the 1D

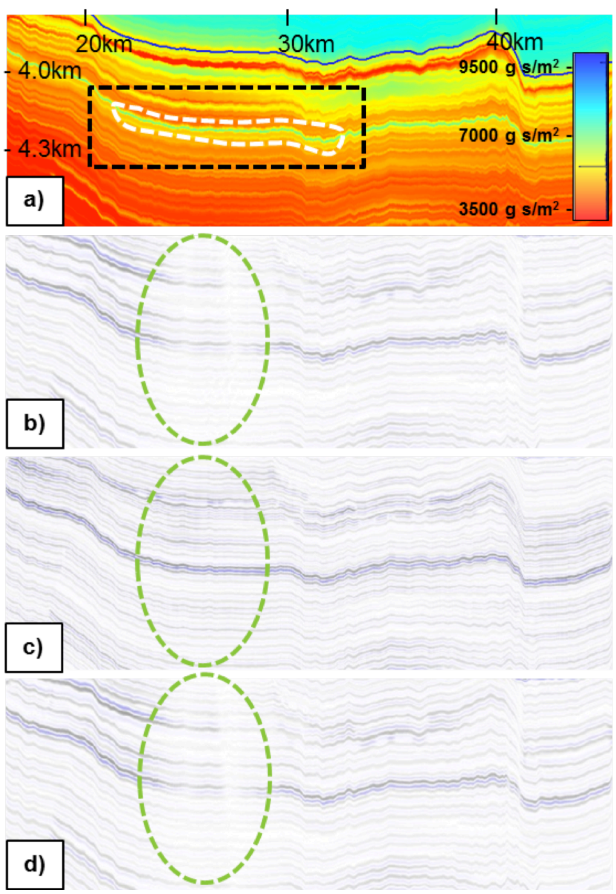

Figure 6 – Impedance model with a small perturbation (3%) in the area around the thin reservoir indicated by the white dashed line (a), image obtained using RTM (b), 1D convolutional forward modeling (c), and PSF-based forward modeling (d).

convolution using a stationary wavelet and the PSF-based forward modeling, respectively. When comparing both methods to the RTM image (cf. Figure 4b), it is clear that the PSF-based forward modeling accurately models both the illumination variations as well as the changes in resolution due to the changes in wavelength. Of course the 1D convolution cannot model any illumination variations as it is not aware of the salt in the overburden. Furthermore, because 1D convolution was here done using a stationary wavelet, it is unable to model any differences in resolution due to changes in wavelength.

To further highlight the ability from the PSF-based forward modeling to capture the illumination variations, we extracted the amplitude along a thin reservoir indicated by the black lines in Figure 4a. The amplitudes are shown in Figure 5 for the RTM image (black line), the 1D convolution (blue line) and the PSF-based forward modeling (red line). Clearly the amplitude resulting from the PSF-based forward modeling accurately captures the illumination variations present in the RTM image, while the 1D convolutional method does not.

The ability of the PSF-based forward modeling to model the illumination variations is expected to be useful for time-lapse feasibility studies. In this case, one wishes to know the impact on the seismic image from a change in the reservoir parameters. In order to simulate this, we slightly perturbed (3%) the impedance model in a small area around the thin reservoir (see the dashed white line in Figure 6a). In order to further test the ability from the PSF-based forward modeling to model illumination variations, a "platform" obstruction was simulated as an

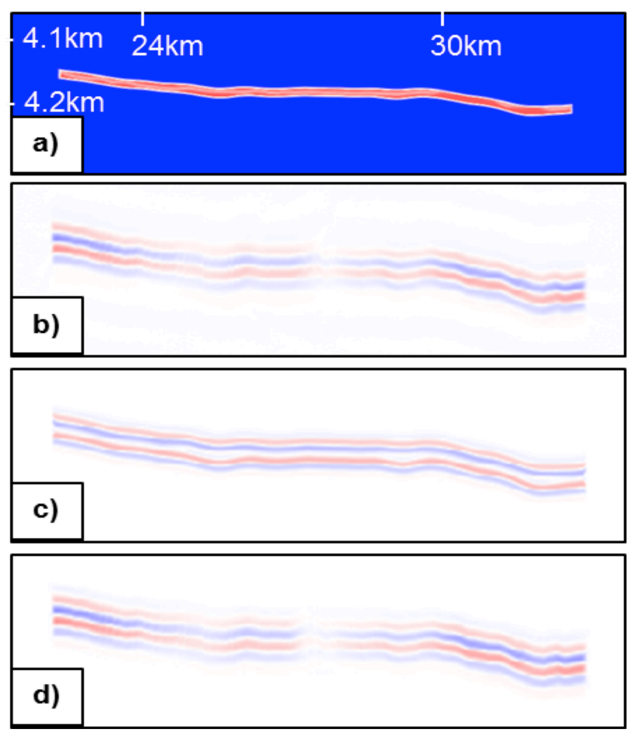

Figure 7 – 3% impedance perturbation in the thin reservoir around the area indicated by the white dashed line in Figure 6 (a), image perturbation from RTM (b), 1D convolution (c) and PSF-based forward modeling.

area without any sources or receivers (see Figure 1). In this way illumination differences due to acquisition variations are introduced on top of illumination variations due to the salt body, i.e. due to the velocity model. Comparing Figures 6b, 6c and 6d, it is clear that the PSF-based forward modeling now accurately captures both illumination variations due the acquisition geometry and the velocity model, while the 1D convolutional method does not. The resulting time-lapse differences in Figure 7 shows the same result. The image perturbation from the 1D convolutional method not only has the wrong wavelength, i.e. wrong resolution, but does not capture any illumination variations. We mention that due to the local nature of the PSF, forward modeling can be done by updating the image only in places where the reflectivity changes.

Discussion

The velocity model used contains mostly mild velocity variations. Combined with the perturbation in the acquisition geometry, however, the modeled data contained substantial illumination variations and the interpolation of the PSFs was able to accurately interpolate these (see Figures 2 and 3). It should be noted, however, that we did not consider what happens close to salt-sediment boundaries where we will encounter sharp velocity contrasts. We anticipate that close to such sharp boundaries the interpolation will be more challenging. The current interpolation method is not limited to 2D and can be extended to 3D.

Conclusions

Using 2D synthetic examples we have shown that post-stack seismic images can be modeled using a weighted sum of PSFs. The PSFs have been calculated using two-way wave-equation-based methods, and as such can efficiently forward model images from a (changing) reflectivity model as if they were obtained using RTM. Therefore, when using this forward modeling in reservoir characterization studies where the field data is migrated using RTM, the reservoir characterization becomes indeed imaging-consistent.

We have demonstrated that the method allows to accurately model illumination variations due to either a complex velocity model or the acquisition geometry. Furthermore it is able to capture resolution variations due to velocity variations in the model. As such the method is superior to the conventional 1D convolutional method that is not able to capture any such variations. We have confirmed these results in a time-lapse setting. Therefore the PSF-based forward modeling will benefit time-lapse feasibility studies for the pre-salt reservoirs offshore Brazil, where the targets are buried underneath a complex overburden and often illuminated using different, not necessarily repeatable, acquisition geometries.

Acknowledgments

We would like to thank Jean-Philippe Coulon for his help in generating the synthetic model, CGG for granting permission to publish this work, and Gerson Ritter from PETROBRAS for several helpful discussions.

References

ALLO, F., RIFFAULT, D., DOYEN, P., NUNES, J.P., DOS SANTOS, M.S., AND JOHANN, P., 2013, Reducing Turn-Around Time for Time-Lapse Feasibility Studies, 13th International Congress of the SBGf, Rio de Janeiro, Brazil.

ARCHER, S.H., DU. X., AND FLETCHER, R.P., 2013, Amplitude inversion of depth-imaged seismic data from areas with complex geology, abstract of the 75th annual meeting of the EAGE, London, UK

CAPRIOLI, P.B.A., DU, X., FLETCHER, R.P., AND VASCONCELOS, I., 2014, 3D source deghosting after imaging, annual meeting of the SEG, Denver

CAPRIOLI, P.B.A., DU, X., AND FLETCHER, R.P., 2015, Deghosting through depth-domain inversion, 77th annual meeting of the EAGE, Madrid, Spain

FLETCHER, R.P., ARCHER, S., NICHOLS, D. AND MAO, W., 2012, Inversion after depth imaging, annual meeting of the SEG, Las Vegas, USA

FORMENTO, J-L., DOS SANTOS M.S., SANSONOVSKI, R.C., RIBEIRO, N.M.S. AND VASQUEZ, G.F., 2007, 4D Seismic Modeling Workflow Over the Marlim Field, 10th International Congress of the SBGf, Rio de Janeiro, Brazil.

HATCHELL, P., KELLY, S., MUERZ, M., JONES, C., ENGBERS, P., VAN DER VEEKEN, J. AND STAPLES, R., 2002, Comparing time-lapse seismic and reservoir model predictions in producing oil and gas fields, EAGE 64th Conference and Exhibition, Florence, Italy.

HUMPREYS, E., CLAYTON, R.W., AND HAGER, B.H., 1984, A tomographic image of mantle structure beneath southern California, Geophysical Research Letters, Vol. 11, No. 7, p.625-627

LECOMTE, I., 2004, Simulating prestack depth migrated sections, 66th annual meeting of the EAGE, Paris, France

LECOMTE, I., 2008, Resolution and illumination analyses in PSDM: A ray-based approach: The Leading Edge, 27, 650–663.

LECOMTE, I., LAVADERA, P. L., BOTTER, C., ANELL, I. M., BUCKLEY, S. J., EIDE, C. H., GRIPPA, A., MASCOLO, V., AND KJOBERG, S., 2016, 2(3)D convolution modelling of complex geological targets beyond – 1D convolution, First Break, 34, p. 99-107

PARKER, R.L., 1994, Geophysical Inverse Theory, Princeton University Press, Princeton, NJ

LETKI, L.P., TANG, J., INYANG, C., DU, X., AND FLETCHER, R.P., 2015, Depth domain inversion to improve the fidelity of subsalt imaging: a Gulf of Mexico case study, First Break, 33, p. 81-85

TOXOPEUS, G., THORBECKE, J., WAPENAAR, K., PETERSEN, S., SLOB, E., AND FOKKEMA, J., 2008, Simulating migrated and inverted seismic data by filtering a geologic model, Geophysics, 73, T1-T10